A New Application of Multimodality Radiomics Improves Diagnostic Accuracy of Nonpalpable Breast Lesions in Patients with Microcalcifications-Only in Mammography

Authors' Contribution:
Study Design A
Data Collection B
Statistical Analysis C
Data Interpretation D
Manuscript Preparation E
Literature Search F
Funds Collection G

AG 1,2,3 Shujun Chen
D 4 Xiaojun Guan
C 5 Zhenyu Shu
B 1,6,7 Yongfeng Li
B 1,8,9 Wenming Cao
F 4 Fei Dong
A 4 Minming Zhang
G 1,2,3 Guoliang Shao
F 1,10,11 Feng Shao

1 Institute of Cancer and Basic Medicine (ICBM), Chinese Academy of Sciences, Hangzhou, Zhejiang, P.R. China
2 Department of Radiology, Cancer Hospital of The University of Chinese Academy of Sciences, Hangzhou, Zhejiang, P.R. China
3 Department of Radiology, Zhejiang Cancer Hospital, Hangzhou, Zhejiang, P.R. China
4 Department of Radiology, 2nd Affiliated Hospital, Zhejiang University School of Medicine, Hangzhou, Zhejiang, P.R. China
5 Department of Radiology, Zhejiang Provincial People's Hospital, Affiliated People's Hospital of Hangzhou Medical College, Hangzhou, Zhejiang, P.R. China
6 Department of Breast Surgery, Cancer Hospital of The University of Chinese Academy of Sciences, Hangzhou, Zhejiang, P.R. China
7 Department of Breast Surgery, Zhejiang Cancer Hospital, Hangzhou, Zhejiang, P.R. China
8 Department of Breast Oncology, Zhejiang Cancer Hospital, Hangzhou, Zhejiang, P.R. China
9 Department of Breast Oncology, Cancer Hospital of The University of Chinese Academy of Sciences, Hangzhou, Zhejiang, P.R. China
10 Department of Gynecological Oncology, Cancer Hospital of The University of Chinese Academy of Sciences, Hangzhou, Zhejiang, P.R. China
11 Department of Gynecological Oncology, Zhejiang Cancer Hospital, Hangzhou, Zhejiang, P.R. China

Corresponding Authors: Feng Shao, e-mail: shaofeng@zjcc.org.cn, Guoliang Shao, e-mail: shaogl@zjcc.org.cn
Source of support: This work was supported by the Zhejiang Medical Technology & Education grant (2014KYB035 and 2018KY279), the Social Development Project of Zhejiang Public Welfare Technology Application (LGF18H180006) and the Natural Science Foundation of Zhejiang Province (LQ17H160013)

Background: The aim of this study was to assess a radiomic scheme that combines image features from digital mammography and dynamic contrast-enhanced MRI to improve classification accuracy of nonpalpable breast lesion (NBL) with Breast Imaging-Reporting and Data System (BI-RADS) 3-5 microcalcifications-only in mammography.

Material/Methods: This retrospective study was approved by the Internal Research Review and Ethical Committee of our hospital. We included 81 patients who underwent a three-dimensional digital breast X-ray wire positioning for local resection between October 2012 and November 2016. All patients underwent breast MRI and mammography before the treatment, and all obtained pathological confirmation. According to the pathological results, 41 patients with benign lesions were assigned to the benign group and 40 patients with malignant lesions were assigned to the malignant group. We used the random forest algorithm to select significant features and to test the single and multimodal classifiers using the Leave-One-Out-Cross-Validation method. An area under the receiver operating characteristic curve was also used to evaluate its discriminating performance.

Results: The multimodal classifier achieved AUC of 0.903, with a sensitivity of 82.5% and a specificity of 80.48%, which was better than any single modality.

Conclusions: Multimodal radiomics classification shows promising power in discriminating malignant lesions from benign lesions in NBL patients with BI-RADS 3-5 microcalcifications-only in mammography.

MeSH Keywords: Breast Neoplasms • Diagnosis • Mammography

Full-text PDF: https://www.medscimonit.com/abstract/index/idArt/918721

📄 2520   📊 3   📊 3   📖 34

Background

Breast cancer is the most frequently diagnosed cancer and the leading cause of cancer-related death in women [1]. The most commonly used methods for breast cancer screening – digital mammography and ultrasound [2] – have shown an increase from 1/3 to 1/2 in breast cancers diagnosed as nonpalpable breast lesion (NBL) [3,4], which is a kind of small lesion of the mammary gland that can only be detected by imaging examinations. Most of these cases are shown as microcalcifications-only in mammography and appear negative in ultrasound [5]. According to the current standards, BI-RADS 3-5 NBL with >2% likelihood of malignancy requires tissue diagnosis to exclude breast cancer [6]. Unlike the mass lesions, the NBL with BI-RADS 3–5 microcalcifications-only in mammography is neither clinically palpable nor guided by ultrasound. Thus, a highly invasive strategy called three-dimensional digital breast X-ray wire positioning technology is frequently performed to locate the microcalcifications for tissue biopsy or local resection. The disadvantage of this approach is that it causes permanent physical damage and anxiety, and because only 22–50% of these lesions are malignant, there is a high false-positive rate [7,8]. The recently revised recommendations for breast cancer screening have suggested that the overtreatment detected by mammography should also be taken into consideration [9,10]. Therefore, finding a new way to improve diagnostic accuracy is of great importance.

Multimodality evaluation for NBL can increase the diagnostic accuracy of breast cancer [11]. Dynamic contrast-enhanced MRI (DCE-MRI), which is a potentially useful candidate biomarker for determining the indication of stereotactic mammotomy biopsy [12,13], has been shown to supply significant diagnostic information on breast lesions showing suspicious microcalcifications on mammography [14–16]. However, since traditional multimodal diagnosis greatly relies on the radiologists' experience, identifying objective multimodal diagnostic markers would contribute to improving the accuracy of NBL identification.

Radiomics can convert medical images into high-dimensional, mineable data via high-throughput extraction of quantitative features based on the established imaging modes [17]. Thanks to the subsequent machine-learning algorithm, it has great potential to become a promising application for predicting the prognosis of breast cancer [18] and identifying the molecular subtyping [19,20]. Preliminary investigations have used radiomics to discriminate malignant tumors from benign ones by using a single modality [7,21]. We believe that fusing multimodality radiomic features could provide a more comprehensive method to quantitatively measure NBL with microcalcifications-only in mammography.

In the present study, we aimed to verify the value of multimodal radiomics in identifying malignant NBL among BI-RADS 3-5 lesions showing microcalcifications-only in mammography by employing mammography and DCE-MRI data.

Material and Methods

Study population

This retrospective study was approved by the Internal Research Review and Ethics Committee of our hospital. All patient data were anonymized before the data were stored in our research dataset. We enrolled patients who underwent a three-dimensional digital breast X-ray wire positioning for local resection with BI-RADS 3-5 microcalcifications-only in mammography between October 2012 and November 2016 consecutively. All the patients underwent paired breast MRI and mammography before the treatment, and all of them had pathologic reports. In this study, mass with calcifications and irregular distortion with calcifications were excluded. Finally, 81 patients were included in the study. According to pathological results, 41 benign patients were assigned to the benign group, and 40 malignant patients were assigned to the malignant group.

Data acquisition

Mammography images were acquired using the digital mammography units (Hologic Selenia, Danbury, USA). Patients underwent imaging with craniocaudal and mediolateral oblique views.

For DCE-MRI image acquisition, all patients were scanned in the prone position using a 3.0 Tesla MRI scanner (MAGNETOM Verio A Tim System; Siemens Healthcare, Erlangen, Germany) with a dedicated 8-channel double-breast coil (Siemens Healthcare, Erlangen, Germany). Contrast agent (Gadodiamide injection, GE Healthcare, Carrigtohill, Ireland) was injected at a dose of 0.1 mmol/kg using a power injector at a flow rate of 2.5 ml/s, followed by a 20-ml saline flush. DCE-MRI sequence was performed using a T1-weighted three-dimensional axial sequence [flip angle = 12°, TR=8 ms, TE=3.93 ms, NEX=1, thickness=0.8 mm, interval=0 mm, matrix=448×448, FOV=340 mm] before and 5 times after intravenous contrast agent administration, and each phase lasted 38 s.

Lesion segmentation

All images were manually segmented by expert board-certified breast radiologists using ITK-SNAP software (*www.itksnap.org*). Radiologists analyzed all 81 cases separately, and they were blinded to the outcomes.
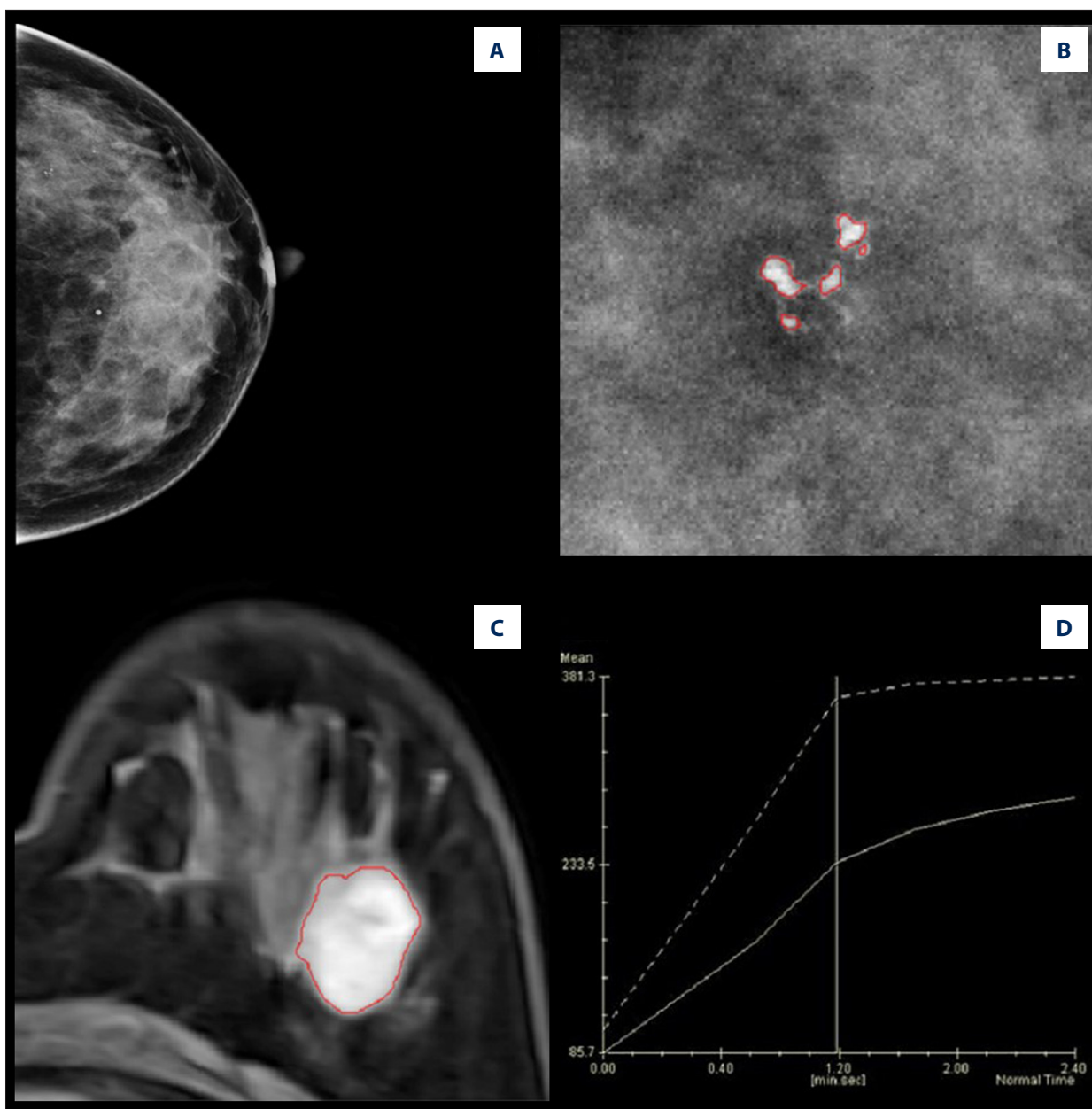
Figure 1. An example of ROI segmentation in the left breast of a patient. (**A**) BI-RADS 4A clustered microcalcifications in the outer quadrant. (**B**) Segmentation on mammography. (**C**) Segmentation on DCE-MRI. (**D**) Dotted lines indicated that the lesion demonstrates kinetics pattern with rapid wash-in.

For lesions in the DCE-MRI image, we segmented the ROI on the DCE-MRI image at the third postcontrast phase, which was closest to 2 min. This was in line with BI-RADS that recommends a morphologic evaluation at the early phase within 2 min [22,23]. The region in the other DCE-MRI phase image was defined as corresponding to the segmented lesion at the third postcontrast phase as a tumor periphery (Figure 1).

Feature extraction

We extracted 3 kinds of corporate features from 2 modalities: morphology features, histogram features, and texture features. In addition, we extracted the characteristic features according to the specific diagnostic value of each modality; from mammography modality we extracted the distribution features of single calcification and the distribution characteristics of single calcification among calcifications clusters, and from DCE-MRI modality we extracted asymmetric features [24] and

Time signal Intensity Curve (TIC) features. All features were extracted by MATLAB software V2018b (*http://www.mathworks.com*). Finally, 69 features of microcalcification were extracted from mammography, including the features of a single calcification and between calcifications. Single calcification features include 9 morphological features, 6 histogram features, and 16 gray-level co-occurrence matrix features. The features between calcifications include 7 distribution features and 31 features regarding heterogeneity between calcifications. We extracted 37 DCE-MRI features, including 11 morphological features, 12 histogram features, 2 texture features, 8 asymmetric features, and 4 time signal intensity curve features. All extracted features are shown in detail in the supplementary materials.

Intra-observer and inter-observer agreement

We evaluated the intra-observer and inter-observer agreements of extracting features by Intra-class Correlation Coefficient (ICC). We first selected 30 random DCE-MRI images for ROI segmentation and feature extraction. The ROI segmentations were performed independently by 2 experienced breast radiologists.

Intra-observer ICC was calculated by comparing 2 extractions of S.G.L. (who has more than 20 years' experience in breast MRI). By comparing the extractions of Z.J. (who has more than 20 years' experience in breast MRI) and the first extraction of S.G.L., Inter-observer was calculated. When the ICC was greater than 0.75, it was considered a good agreement, and the other images segmentation was performed by Z.J.

Feature selection and Classification algorithm

First, we used the random forest-recursive feature elimination method to select the features from each modality separately [24]. We sorted variables according to the characteristics of the descending order of importance, and then deleted the ones with the lowest importance; these same steps were repeated until the feature set was reduced to 1. We evaluated a subset of different features and then chose the minimum out of bag error subset as the chosen features. Then, we used the random forest algorithm, which is an integrated learning algorithm used to build the multimodal classifier. It is a classifier composed of many decision trees, where the output is determined by voting, and the number of votes is classified as the classification result [25]. We used the LOOCV method to validate and improve the generalization ability of the classifiers [26].

Statistical analysis

Statistical differences between the features of malignant and benign lesions were analyzed by using the independent-samples t test. The age differences between the 2 groups were tested using a two-sample t test. ROC analysis was used to

Table 1. Demographic details of subjects.

Pathology	Statistic
Breast cancer (n=40)	
Age in years [mean±SD (range)]	46.67±9.4 (28–68)
Histology type	
	Number
Invasive ductal carcinoma (IDC)	22
Ductal carcinoma *in situ* (DCIS)	16
Invasive mucinous carcinoma	1
Invasive cribriform carcinoma	1
Breast benign lesions (n=41)	
Age in years [mean±SD (range)]	46.51±9.6 (27–59)
Histology type	
	Number
Fibroadenoma	6
Duct ectasia	28
Ductal epithelial hyperplasia	30
Cysts	5
Benign proliferative breast disease	36
Sclerosing adenosis	1
Intraductal papilloma	4

evaluate classifier performance. AUC was used as an index of performance. Statistical analysis was performed using SPSS 17.0 (SPSS, Inc., Chicago, IL, USA). All tests were two-tailed. P<0.05 was considered statistically significant.

Results

Patient characteristics

The mean age of the malignant patients was 46.67±9.4 years (range: 28–68 years), the mean age of the benign patients was 46.51±9.6 years (range: 27–59 years), and all patients were Han Chinese females. There was no significant difference in age between the groups (p>0.05). Also, all malignant patients were early-stage breast cancer. Table 1 shows the histological types and demographic details of these subjects.

Multimodal feature extraction

In this study, 69 candidate radiomics features were reduced to 6 potential mammographic features (Figure 2A), and 37 candidate DCE-MRI features were reduced to 8 potential
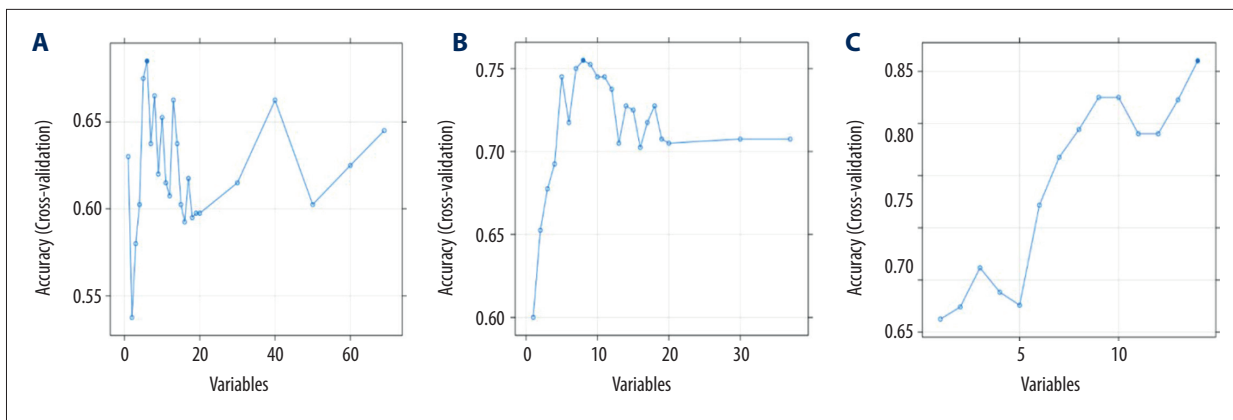
Figure 2. The accuracy curve of the number of features. (**A**) Based on mammography, there is a maximum accuracy when the feature is 6. (**B**) Based on DCE-MRI, there is a maximum accuracy when the feature is 8. (**C**) Based on the extraction features from multimodal, when the total number of features was 14, the accuracy is the highest.

Table 2. Multimodal classification features and statistical significance between malignant and benign lesions.

Characteristic	MG			Characteristic	DCE-MRI		
	Malignant lesion (n=40)	Benign lesion (n=41)	P value		Malignant lesion (n=40)	Benign lesion (n=41)	P value
Heterogeneity between individual calcification				Morphologic features			
F51	1.442±0.641	1,873±0.495	0.031	F70, mm^2	1031±738	1675±2074	0.002
F53	1.561±0.612	1.773±0.327	0.6674	F71, mm	60.3±12.2	72.3±22.5	<0.001
F54	1.453±0.632	1.763±0.465	0.003	F72	0.675±0.035	0.723±0.043	<0.001
F55	6.18±0.28	6.61±0.26	<0.001	Texture features			
Distribution of the calcifications range features				F92	164±28	132±39	0.021
F65	0.0284±0.0026	0.0389±0.0039	<0.001	Time-signal intensity curve features			
F69	0.0325±0.0027	0.0512±0.0041	<0.001	F94	1.01±0.221	1.192±0.182	<0.001
				F95	1.203±0.179	1.538±0.211	<0.001
				F96	1.732±0.221	1.813±0.219	0.8153
				F97	2.145±0.281	2.312±0.283	0.3873

features (Figure 2B). Based on the extraction features from multimodal images, the accuracy was the highest when the total number of features was 14 (Figure 2C). The contrast texture features (3/6) in mammography and the kinetic features in DCE-MRI (4/8) were the most discriminative features in joining the 2 modalities (Table 2). In mammography, there were significant differences between malignant lesions and benign lesions in some texture features, including the variance of the contrast of the grayscale co-occurrence matrix at 0° (P=0.031), grayscale co-occurrence matrix at 135° (P=0.003), and the variance of the energy of the grayscale co-occurrence matrix

at 0° (P<0.001). In distribution of the calcifications range features such as SD of the distance of the calcification spot from the center (P<0.001), the maximum distance between the calcification spots in the area of the radius 0.5 cm (P<0.001). In DCE-MRI, there were significant differences between morphologic features such as circumference (P<0.001), area (P=0.002), roundness (P<0.001), the slope of the fitting of the first 3 points of the time signal intensity curve (P<0.001), the slope of the fitting of the first 4 points of the time signal intensity curve (P<0.001), and the texture feature largest variance (P=0.021).

Table 3. ROC curve analysis of single modality and multimodality parameters for assessment of the performance of the classifier.

Modality	Sensitivity	Specificity	AUC	Accuracy
Mammography	77.50%	73.17%	0.834	75.30%
DCE-MRI	75.00%	78.04%	0.883	76.54%
Mammography+DCE-MRI	82.50%	80.48%	0.903	81.48%
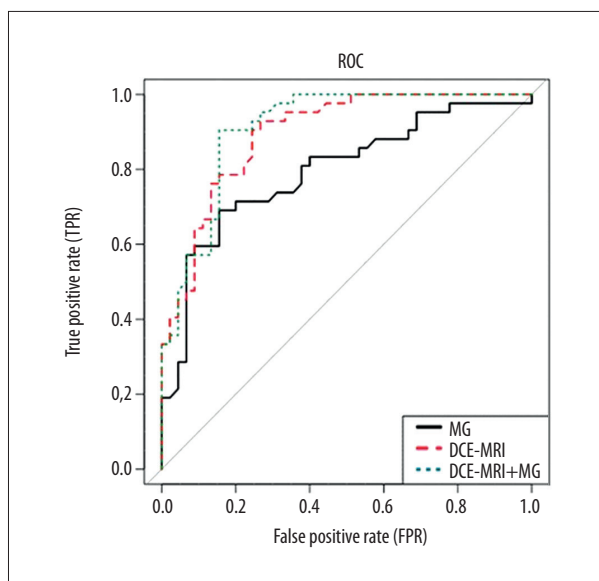
Figure 3. The ROC curve of single modality and multimodality. MG – mammography.

The performance of multimodal classifier

We used the random forest-recursive feature elimination method to build the multimodal classifier. Our model achieved AUC 0.903, with a sensitivity of 82.5%, a specificity of 80.48%, and a classification accuracy of 81.48%, which was better than with any single model, and which indicated good diagnostic power. The classification performance of the combined features is listed in Table 3. The performance of the Receiver Operating Characteristics (ROC) curve is shown in Figure 3.

Intra-observer reproducibility and inter-observer variability analysis

The intra-observer ICC calculated based on 2 measurements of S.G.L. ranged from 0.802 to 0.978. The inter-observer agreement between 2 breast radiologists ranged from 0.781 to 0.925. The results indicated good intra- and inter-observer feature extraction reproducibility.

Discussion

Mammography and DCE-MRI are 2 modalities that strongly complement each other in the differentiation of patients with malignant and benign NBL with microcalcifications-only in mammography. Mammography has high specificity for microcalcifications but low tissue contrast, while MRI has high resolution, high sensitivity (78–98%), and low specificity (43–75%) in soft tissue [27]. Even though joining radiomic features from mammography and DCE-MRI is not an easy task in NBL with microcalcifications-only because the signs are atypical in both modalities, some atypical localized breast adenopathies can also show similar morphology microcalcifications in the ducts, like the malignant ones in mammography. Most MRI findings are non-mass-like enhancements, and the sensitivity and specificity of DCE-MRI are, in general, much lower for the diagnosis of non-mass-like enhancement lesions compared with masses [28,29]. Previous multimodality computer-aided breast cancer diagnosis based on these 2 modalities has shown the improvement of single-modality mammography (AUC 0.74±0.04), DCE-MRI (AUC 0.78±0.04) to multimodality (AUC 0.87±0.03), but they only focused on the mass [30]. Our results were different from previous reports since our study population specifically focused on NBL patients with microcalcifications-only. This kind of disease cannot be found in other commonly used screening methods and is more difficult to diagnose and to treat. We excluded the masses with calcifications, spiculation with calcifications, and architectural distortion with microcalcifications because these 3 kinds of diseases are palpable and can be localized with ultrasound. Above all, our results demonstrated that combining radiomic information from these 2 modalities had good diagnostic power and led to higher performances in accuracy, sensitivity, specificity, and AUC than with any single modality alone.

In our study, we found that the contrast texture feature in mammography and the kinetic features in DCE-MRI were the significant differentiators of malignant lesions from benign lesions in NBL patients with microcalcifications-only. We found that in mammography, the malignant lesions had significantly less clarity and groove of the image textures than benign lesions, and their texture was irregular and unstable compared to the benign lesions. We also found the malignant calcifications had more intensively clustered distribution. These differences may correspond to the way malignant microcalcifications

appear on the mammogram as either linear, branching, or granular microcalcifications, which are usually coarse and are usually distributed as multiple clusters of fine granular microcalcifications [31]. In another modality – DCE-MRI – we found that the malignant lesions had significantly smaller circumference and area, with no smooth edges. This difference may correspond to the appearance of ductal carcinoma, which is amorphous, depending primarily on the presence and extent of abnormal periductal or stromal vascularity. In this type of cancer, the invasive tumor tissue is densely distributed along the duct [32]. The malignant lesions had a higher enhancing slope rate, which may correspond to the immature blood vessels in the tumor. More enhanced heterogeneity in the malignant lesions may be correlates with the higher heterogeneity in tumors.

We used the random forest algorithm to select the features and build the classifiers. We performed encapsulated feature selection to build a classifier combination method. This approach can eliminate the uncorrelated or redundant features, thus reducing the number of features, improve the accuracy of the model, and reduce the running time [33]. It can also enable better predictive performance and model interpretation than variable selection by Least Absolute Shrinkage and Selection Operator (LASSO) [34]. Our radiomics data were collected from a single institution, using the same equipment and protocol, thus eliminating the effects of inconsistent data on results.

Our study suggests that an appropriate quantitative scheme can reduce the false-positive rate and adjust thresholds for image-guided breast biopsy. Our results show that adding MRI examination will improve the sensitivity, specificity, AUC, and accuracy compared with the single use of mammography in the diagnosis of NBL. In light of the current high incidence of breast cancer, this will result in considerable clinical benefits.

The reported results may help improve the selection process for the patients with NBL and BI-RADS 3-5 appearing as microcalcifications-only at mammography before any highly invasive strategies are used.

Our study has several limitations. First, our study was retrospective, which means that it was subjected to potential bias. Second, we had a small data set, since breast MRI is still not the routine examination for most patients with NBL calcifications-only. Third, the clinical risk factors were not incorporated. Further large-scale studies are needed to confirm our findings and to potentially identify a cutoff value with radiomics that should be used to optimize the selection of patients who will benefit from preoperative breast MRI.

Conclusions

The quantitative multimodal radiomic diagnostic model is a promising method for diagnosing NBL patients with BI-RADS 3-5 microcalcifications-only. This method has the potential to become an essential diagnostic procedure and a reliable approach for clinical strategy pre-treatment. Breast MRI imaging is potentially useful to predict the presence of occult invasion in patients with suspicious calcifications.

Ethics statement

Approval for retrospective chart review was obtained from the Institutional Review Board (IRB), and HIPPA compliance was strictly adhered to ([2014]-05-42).

Conflicts of interest

None.

References:

1. Bray F, Ferlay J, Soerjomataram I et al: Global cancer statistics 2018: GLOBOCAN estimates of incidence and mortality worldwide for 36 cancers in 185 countries. Cancer J Clin, 2018; 68: 394–424

2. Lehman CD, Wellman RD, Buist DS et al., Breast Cancer Surveillance Consortium: Diagnostic accuracy of digital screening mammography with and without computer-aided detection. JAMA Intern Med, 2015; 175: 1828–37

3. (HSCIC) HaSCIC. Breast Screening Programme[online] England 2013–2014; http://www.hscic.gov.uk/article/2021/Website-Search?productid= 17263&q= breast+cancer+screening+&sort= Relevance&size=10&page=1&area=both

4. Netherlands Centre for Population Screening BCSP. Breast Cancer Screening Programme[online]. http://wwwrivmnl/dsresource?objectid=rivmp: 273146&type=org&disposition=inline&ns_nc=1

5. Bassett LW: Mammographic analysis of calcifications. Radiol Clin North Am, 1992; 30: 93–105

6. Kim SY, Kim HY, Kim EK et al: Evaluation of malignancy risk stratification of microcalcifications detected on mammography: A study based on the 5th edition of BI-RADS. Ann Surg Oncol, 2015; 22: 2895–901

7. Bickelhaupt S, Paech D, Kickingereder P et al: Prediction of malignancy by a radiomic signature from contrast agent-free diffusion MRI in suspicious breast lesions found on screening mammography. J Magn Reson Imaging, 2017; 46(2): 604–16

8. Michel SC, Low R, Singer G et al: Stereotactic mammotome breast biopsy: Routine clinical experience and correlation with BI-RADS – classification and histopathology. Praxis (Bern 1994), 2007; 96: 1459–74

9. Siu AL: Screening for breast cancer: U.S. Preventive Services Task Force Recommendation Statement. Ann Intern Med, 2016; 164: 279–96

10. Oeffinger KC, Fontham ET, Etzioni R et al: Breast cancer screening for women at average risk: 2015 guideline update from the American Cancer Society. JAMA, 2015; 314: 1599–614

11. Shin HJ, Kim HH, Ahn JH et al: Comparison of mammography, sonography, MRI and clinical examination in patients with locally advanced or inflammatory breast cancer who underwent neoadjuvant chemotherapy. Br J Radiol, 2011; 84: 612–20

12. Brnic D, Brnic D, Simundic I et al: MRI and comparison mammography: A worthy diagnostic alliance for breast microcalcifications? Acta Radiol, 2016; 57: 413–21

13. Kikuchi M, Tanino H, Kosaka Y et al: Usefulness of MRI of Microcalcification Lesions to Determine the Indication for Stereotactic Mammotome Biopsy. Anticancer Res, 2014; 34: 6749–53

14. Stehouwer BL, Merckel LG, Verkooijen HM et al: 3-T breast magnetic resonance imaging in patients with suspicious microcalcifications on mammography. Eur Radiol, 2014; 24: 603–9

15. Li E, Li J, Song Y et al: A comparative study of the diagnostic value of contrast-enhanced breast MR imaging and mammography on patients with BI-RADS 3-5 microcalcifications. PLoS One, 2014; 9: e111217

16. Jiang Y, Lou J, Wang S et al: Evaluation of the role of dynamic contrast-enhanced MR imaging for patients with BI-RADS 3-4 microcalcifications. PLoS One, 2014; 9: e99669

17. Parekh V, Jacobs MA: Radiomics: A new application from established techniques. Expert Rev Precis Med Drug Dev, 2016; 1: 207–26

18. Li H, Zhu Y, Burnside ES et al: MR imaging radiomics signatures for predicting the risk of breast cancer recurrence as given by research versions of MammaPrint, Oncotype DX, and PAM50 gene assays. Radiology, 2016; 281: 382–91

19. Wang J, Kato F, Oyama-Manabe N et al: Identifying triple-negative breast cancer using background parenchymal enhancement heterogeneity on dynamic contrast-enhanced MRI: A pilot radiomics study. PLoS One, 2015; 10: e0143308

20. Li H, Zhu Y, Burnside ES, Huang E et al: Quantitative MRI radiomics in the prediction of molecular classifications of breast cancer subtypes in the TCGA/TCIA data set. NPJ Breast Cancer, 2016; 2: pii: 16012

21. Bickelhaupt S, Steudle F, Paech D et al: On a fractional order calculus model in diffusion weighted breast imaging to differentiate between malignant and benign breast lesions detected on X-ray screening mammography. PLoS One, 2017; 12: e176077

22. American College of Radiology: Breast imaging reporting and data system (BI-RADS), 5th edition: American College of Radiology, 2013

23. Agrawal G, Su MY, Nalcioglu O, Feig SA, Chen JH: Significance of breast lesion descriptors in the ACR BI-RADS MRI lexicon. Cancer, 2009; 115: 1363–80

24. Granitto PM, Furlanello C, Biasioli F et al: Recursive feature elimination with random forest for PTR-MS analysis of agroindustrial products. Chemometrics and Intelligent Laboratory Systems, 2006; 83: 83–90

25. Liaw A, Wiener M: Classification and regression by randomforest. R News, 2002; 23: 23

26. A study of cross-validation and bootstrap for accuracy estimation and model selection. International Joint Conference on Artificial Intelligence. Morgan Kaufmann Publishers Inc., 1995; 1137–43

27. Kuhl CK: Current status of breast MR imaging. Part 2. Clinical applications. Radiology, 2007; 244: 672–91

28. Newstead GM: MR imaging of ductal carcinoma *in situ*. Magn Reson Imaging Clin N Am, 2010; 18: 225–40, viii

29. Goto M, Ito H, Akazawa K et al: Diagnosis of breast tumors by contrast-enhanced MR imaging: Comparison between the diagnostic performance of dynamic enhancement patterns and morphologic features. J Magn Reson Imaging, 2007; 25: 104–12

30. Yuan Y, Giger ML, Li H et al: Multimodality computer-aided breast cancer diagnosis with FFDM and DCE-MRI. Acad Radiol, 2010; 17: 1158–67

31. Holland R, Hendriks JH: Microcalcifications associated with ductal carcinoma *in situ*: Mammographic-pathologic correlation. Semin Diagn Pathol, 1994; 11: 181–92

32. Yamada T, Mori N, Watanabe M et al: Radiologic-pathologic correlation of ductal carcinoma *in situ*. Radiographics, 2010; 30: 1183–98

33. Yao D, Yang J, Zhan X et al: A novel random forests-based feature selection method for microarray expression data analysis. Int J Data Min Bioinform, 2015; 13: 84–101

34. Zhu XW, Xin YJ, Ge HL: Recursive random forests enable better predictive performance and model interpretation than variable selection by LASSO. J Chem Inf Model, 2015; 55: 736–46